Characterisation of a gel in the cell wall to elucidate the paradoxical shrinkage of tension wood

Bruno Clair, Joseph Gril, Francesco Di Renzo, Hiroyuki Yamamoto, Françoise Quignard

Characterization of a Gel in the Cell Wall To Elucidate the Paradoxical Shrinkage of Tension Wood

Bruno Clair,*,† Joseph Gril,† Francesco Di Renzo,‡ Hiroyuki Yamamoto,§ and Françoise Quignard‡

Laboratoire de Mécanique et Génie Civil (LMGC), Université Montpellier 2, CNRS, 34095 Montpellier, France, Institut Charles Gerhardt Montpellier, CNRS, Université Montpellier 2, ENSCM, Université Montpellier 1, 34296 Montpellier, France, and School of Bioagricultural Sciences, Nagoya University, Nagoya 464-8601, Japan

Wood behavior is characterized by high sensibility to humidity and strongly anisotropic properties. The drying shrinkage along the fibers, usually small due to the reinforcing action of cellulosic microfibrils, is surprisingly high in the so-called tension wood, produced by trees to respond to strong reorientation requirements. In this study, nitrogen adsorption–desorption isotherms of supercritically dried tension wood and normal wood show that the tension wood cell wall has a gel-like structure characterized by a pore surface more than 30 times higher than that in normal wood. Syneresis of the tension wood gel explains its paradoxical drying shrinkage. This result could help to reduce technological problems during drying. Potential applications in biomechanics and biomimetics are worth investigating, considering that, in living trees, tension wood produces tensile growth stresses 10 times higher than that of normal wood.

1. Introduction

Two conditions allow trees to grow higher than other plants. The most obvious one is the secondary diameter growth of their stems, through production of successive wood layers by the peripheral cambium. The combination of honeycomb-like cellular organization and multilayering of the cell wall makes wooden tissues highly efficient to support high axial load. Figure 1 shows the typical structure of a normal wood cell, with the secondary layer divided into sublayers with different microfibrillar angles (MFAs), a parameter describing the inclination of crystalline cellulose relative to the cell axis. A less visible but equally important condition is the prestressing resulting from the cellular maturation, which not only improves the strength of the stem but also controls its orientation through the asymmetry of growth and stress distribution.[1,2] In the case of strong reorientation requirements, a so-called reaction wood is produced, characterized by distinctive anatomical features and biomechanical action. In softwoods the lower part of a leaning stem would produce a tissue that tends to expand during maturation and is thus subject to compression stress.[3] Compared to normal wood (NW), the tracheids of this "compression wood" are more lignified and their S_2 layer has a high MFA. As a result, the cell wall is less rigid and this usually needs to be compensated by the production of denser wood and larger growth rings.[3] By contrast, the "tension wood" (TW), located on the upper side of leaning stems in hardwoods, tends to contract during maturation and generates a high tension. Although several types of tension wood have been reported,[4] they all contain more cellulose,[5] exhibit low MFAs,[6,7] and seem to be extremely efficient in terms of biomechanical action.[8] In many species, a part of the secondary wall is replaced by a distinctive layer (Figure 1). This layer was discovered by Th. Hartig at the end of the 19th century and is named the cellulosic layer, mucilaginous layer, cartilaginous layer, or gelatinous layer because of its cellulose content, detachment from other layers, and jelly-like appearance.[9–13] Later and until now, the scientific community adopted the name "gelatinous layer" (G-layer) although its structure is described as purely or highly cellulosic, highly crystalline,[5] and with very low or nil MFA.[6] Fast growing plantation species of increasing commercial importance like some eucalypt clones and poplar do contain typical gelatinous fibers; it is likely that in the future they will represent a significant proportion of the biomass produced by these forests.

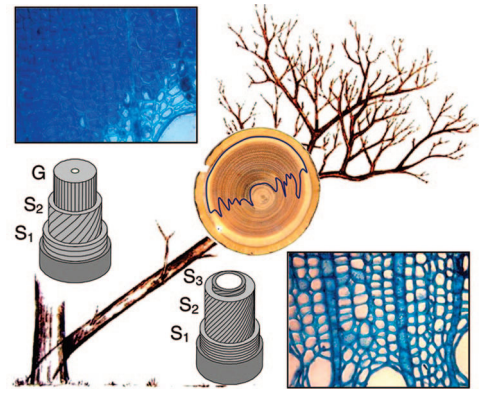

Figure 1. Drawing of the sampled tree and photo of its cross section (6 cm diameter) with tension wood (TW) shown on the upper side. Photos of transverse sections (width 380 μm) stained with O-Toluidine Blue and a schematic representation of the multilayer ultrastructure and associated microfibril angle in TW cell wall (above) compared to normal wood (NW) (below). In NW the low MFA of the thicker S_2 sublayer reinforces the axial direction, while the high MFA in S_1 and S_3 provides transverse stability. In TW, a part of S_2 has been replaced by G and S_3 no longer exists.

* To whom correspondence should be addressed. Phone: (33) 4 6714 4918. Fax: (33) 4 6714 4792. E-mail: clair@lmgc.univ-montp2.fr.

† Laboratoire de Mécanique et Génie Civil, Université Montpellier 2, CNRS.

‡ Institut Charles Gerhardt CNRS, Université Montpellier 2, ENSCM, Université Montpellier 1.

§ School of Bioagricultural Sciences, Nagoya University.

This is not, however, good news for the wood industry, as tension wood is generally regarded as a major defect. The release of prestresses leads to log-end cracks and lumber distortion while the wood remains green; in the later stages of wood drying and use in products, the difference in physical properties between normal and reaction woods is likely cause severe problems.

A most striking property of G-fiber tension woods is their large longitudinal shrinkage. In normal wood, the departure of bound water results in anisotropic shrinkage, typically 0.05−0.3% along the grain (L direction), 3−6% in radial (R), and 6−12% in tangential (T) directions.[14] As a general trend, the lower the MFA, the lower the L shrinkage; this can be easily explained by the reinforcing action of the crystalline microfibrils that resist water-induced movements along their length.[15–18] It is therefore surprising to observe a large L shrinkage exceeding 1% in tension woods where the MFA is the smallest.[19–22] Norberg and Meier,[5] who observed isolated portions of the G-layer, reported that they do not exhibit high longitudinal shrinkage. The G-layer is generally loosened from the S_2 layer and this latter one is very thin in tension wood. So these authors and Boyd[23] assumed that, in that case, longitudinal shrinkage is produced by the high microfibril angle in the S_1 layer, with the G-layer being unable to prevent it. Some years ago, however, thanks to new observation techniques such as atomic force microscopy, experimental evidence of G-layer shrinkage was produced.[24] A model demonstrating the necessity of G-layer shrinkage to explain macroscopic longitudinal shrinkage was proposed,[22,25] and the shrinkage of some amorphous part of the cellulose microfibrils was hypothesized. Recent observations of a cutting artifact in G-layer[26,27] evidenced the weak bonding between microfibrils transversally to the fiber axis. X-ray diffraction experiments proved that cellulose microfibrils are very lightly shortened during axial drying shrinkage compared to the macroscopic L shrinkage. These observations led to the conclusion that G-layer cellulose is subject to buckling during drying shrinkage and cannot be its active agent.[28] The origin of G-layer shrinkage is then still a matter of debate.

In addition to this large shrinkage, drying induces in G-fiber tension woods an exceptional level of rigidification. From the green to oven-dry state, a rigidity ratio higher than 2 has been observed in TW containing G-layer, whereas it amounts to typically 1.3 in other wood types. As gels are known to be highly rigidified during drying,[29] these features strongly suggest the existence of gel-like structures in G-layers, which had never been referred before. The objective of this study is to check this assumption through porosity measurements in the wet and dry states by nitrogen adsorption−desorption isotherms.

2. Material and Methods

Experiments have been performed on chestnut wood (Castanea sativa Mill.). A 20 year old tilted tree was chosen, and wood samples were extracted from both sides of the trunk: tension wood on the upper side and normal wood on the lower side (Figure 1). Chestnut is known to produce TW with a typical G-layer and to exhibit high longitudinal shrinkage and stiffness increase during drying compared to normal wood (NW).[20] Color contrast allowed us to localize clearly TW on a wood disk cut from the upper side of the trunk (Figure 1); anatomical observation with optical microscopy confirmed the presence of a thick G-layer (Figure 1). NW (without a G-layer) was used as reference to ensure that the observed phenomenon can only be attributed to the G-layer.

Wood samples were divided in two paired sample sets. One set of samples was dried by heating at 102 °C during 72 h in a ventilated oven (evaporation dried samples). The other set was supercritical dried (aerogel samples).

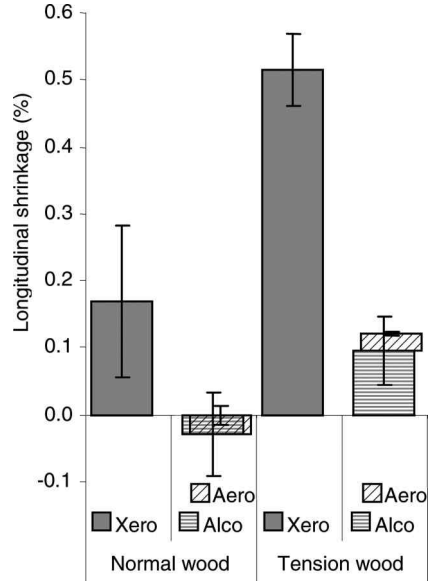

Figure 2. Longitudinal shrinkage of samples of normal (NW) and tension (TW) chestnut wood upon oven drying (Xero), ethanol exchange (Alco), and supercritical CO_2 drying (Aero). (Negative values correspond to swelling.)

Supercritical Drying. The aerogel samples were prepared by immersion of the wood samples in a series of successive ethanol–water baths of increasing alcohol concentration (30, 60, 90, 100% three times) during 24 h each. The dehydrated samples were introduced in a Polaron 3100 apparatus which was then filled with liquid CO_2. Samples stay 2 h in liquid CO_2 before ethanol evacuation. Temperature was raised to 32 °C so that CO_2 reaches its critical point (74 bar, 31.5 °C). Depressurization took 35 min. In this way, the shrinkage due to capillary pressure is prevented and the aerogel formed is expected to reproduce in the dry state the texture of the original hydrogel.[30,31] In this treatment, water is replaced by a solvent which is then extracted beyond its critical point. In the case of polysaccharide gels, alcohol exchange and CO_2 supercritical drying have proved to be efficient methods to preserve the volume and the microscopical texture of the gel.[32,33]

Macroscopic Longitudinal Shrinkage. Measurements were performed on samples (55 mm long and 2 mm thick) taken from the same tree (8 NW and 12 TW) and divided into two sets: one oven-dried and the other critical dried. On each sample, the length in wet condition (L_W) and the length in dry conditions (L_D) were measured using a digital micrometer (0.001 mm precision). Macroscopic longitudinal shrinkage was calculated as $LS = (L_W - L_D)/L_W$.

Scanning Electron Microscopy. Supercritical dried tension wood samples have been observed by scanning electron microscopy (SEM, Hitachi S-4500) on longitudinal sections after platinum metallization. The size of the aggregates of fibrils has been measured normally to the fibril axes using ImageJ image analysis freeware.[34]

Surface Area and Porosity. Nitrogen adsorption–desorption isotherms were recorded at 77 K on a Micromeritics ASAP 2010 volumetric apparatus. Prior to the adsorption experiment, samples were outgassed in situ at 323 K until a static vacuum of 0.6 Pa was reached. Nitrogen doses were admitted, and the adsorbed amount was registered as a function of the equilibrium pressure (Figure 2). The surface area of the sample was measured by the BET method, which allows evaluation of the amount of adsorbate corresponding to a molecular monolayer.[35]

3. Results and Discussion

Macroscopic shrinkage measurements for the oven-dried sample (xerogel) and the supercritically dried sample (aerogel)

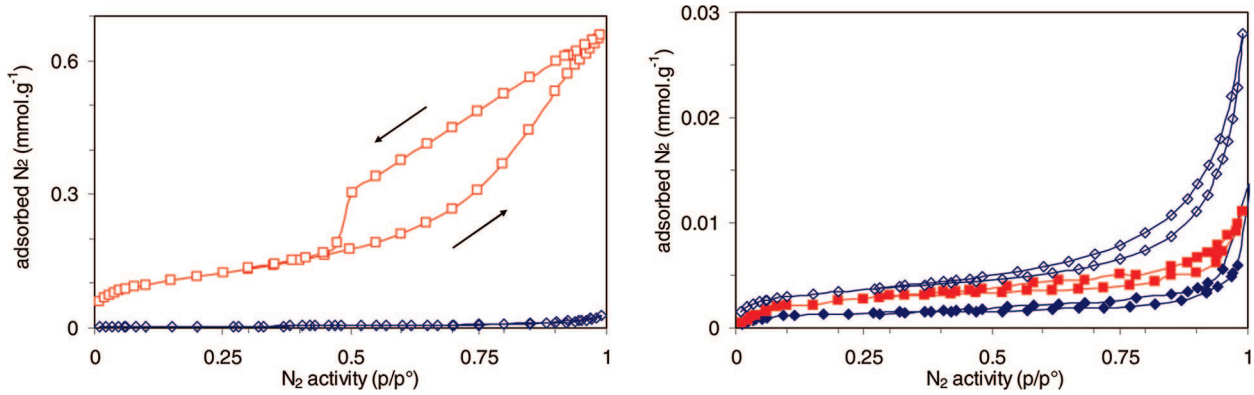

Figure 3. N_2 adsorption–desorption isotherms: (left) aerogel of tension wood (TW) and normal wood (NW); (right) NW and TW xerogel compared to NW aerogel. Key: square, TW; diamond, NW; void shapes, aerogel; filled shapes, xerogel.

are reported in Figure 2. Longitudinal shrinkage between alcogel and aerogel amounted to about 0.03% in both NW and TW, a very low figure compared to oven drying where the shrinkage was measured as 0.18% in NW and 0.52% in TW. However, it has to be noticed that the exchange from water to alcohol induced some minor modifications: 0.03% swelling for NW (later compensated by the shrinkage during the critical drying) and 0.11% shrinkage for TW. Nevertheless, the measured shrinkages confirm the effectiveness of supercritical drying to prevent most of the deformation of the wood samples.

Examples of nitrogen adsorption–desorption isotherms of TW and NW aerogels and xerogels are reported in Figure 3 (four other isotherms of TW were performed for confirmation and similar isotherms were observed). It is evident from Figure 3 that the TW aerogel adsorbs a much larger amount of nitrogen than the NW aerogel. The amount of nitrogen needed to form a monolayer of adsorbed molecules provides a good estimate of the surface area of the sample. For our samples it nearly corresponds to the amount adsorbed at $p/p° = 0.1$ and is more than 30 times higher for the TW aerogel compared to the NW aerogel, yielding surface areas of 18.8 $m^2\ g^{-1}$ for TW and 0.56 $m^2\ g^{-1}$ for NW. The isotherms of evaporatively dried TW and NW are similar to the isotherm of NW aerogel with surface areas lower than 0.5 $m^2\ g^{-1}$. Supercritically dried TW presents a high surface area which is completely lost when the same wood is evaporatively dried. In NW, very low surface areas are observed in both the evaporatively and supercritically dried samples.

The high surface area of the TW aerogel is accompanied by a significant porosity. The isotherm reported in Figure 3 is type IV according to the classification of IUPAC,[36] presenting the hysteresis loop typical of mesoporous adsorbents, viz., adsorbents with pores whose diameter is between 2 and 50 nm. The average mesopore size can be evaluated from the relative pressure at which capillary condensation takes place. The maximum slope of the adsorption isotherm corresponds to a pore diameter of nearly 7 nm.[37] The wide hysteresis loop between the adsorption and desorption branches of the isotherm indicates that the pores present an ink-bottle shape, viz., the pore opening is somewhat narrower than the pore body. The sudden desorption near $p/p° = 0.48$ is a cavitation phenomenon and indicates that the opening of a fraction of the mesopores is smaller than about 4 nm.[38]

More information about the nature of the porosity can be drawn from the *t*-plot transform of the adsorption isotherm on the TW aerogel, which is reported in Figure 4. The linear extrapolation of the initial part of the transform passes through the origin, indicating that no micropores (pores with diameter

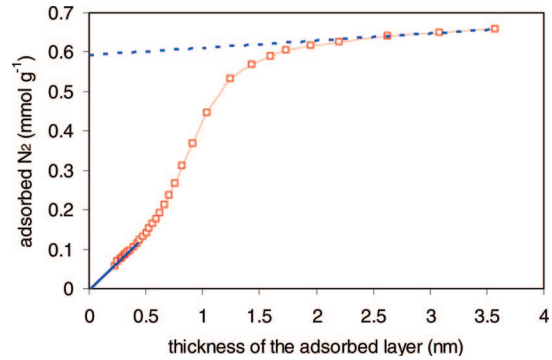

Figure 4. *t*-plot of the adsorption of N_2 at 77 K on aerogel of tension wood.

smaller than 2 nm) are present. The slope of the initial linear part of the transform is proportional to the surface area. The evaluation of the surface area by comparison of this slope with the slope measured on a reference sample of known surface provides a result in excellent agreement with the BET method. When the statistical thickness of the adsorbed layer is larger than about 0.5 nm, the slope of the *t*-plot increases and the transform is no longer linear. This indicates that the adsorption due to capillary condensation in the mesopores is overcoming the layer-by-layer adsorption on the surface. Capillary condensation continues until the activity of N_2 corresponds to the adsorption of a 3 nm thick layer. The final part of the *t*-plot is linear and corresponds to a layer-by-layer adsorption. The slope of the linear correlation indicates that, once the mesopores are filled, the outer surface area of the mesoporous adsorbent is about 1.3 $m^2\ g^{-1}$. The extrapolation at zero thickness of the linear correlation allows evaluation of the mesopore volume, 0.04 $cm^3\ g^{-1}$. It has to be recalled that N_2 adsorption does not allow observation of pores larger than about 50 nm.

It is especially significant that the NW sample presents very little porosity or surface area when supercritically dried. This allows us to attribute virtually the whole surface area of the TW sample to the component which differentiates it from NW, viz., the G-layer.

The area ratio between G-layers and other layers was measured as 50% by SEM on supercritical dried samples. Transverse shrinkage in G-layer during drying has been measured in a previous work as around 20%.[39] Considering the disappearance of pores during drying (as proved by the evaporative dried TW isotherm), the oven dry state allows measurement of the amount of dense microfibrils. The mass fraction of G-layer in the TW sample has then been evaluated to about 39%. As a consequence, the G-layer can be considered

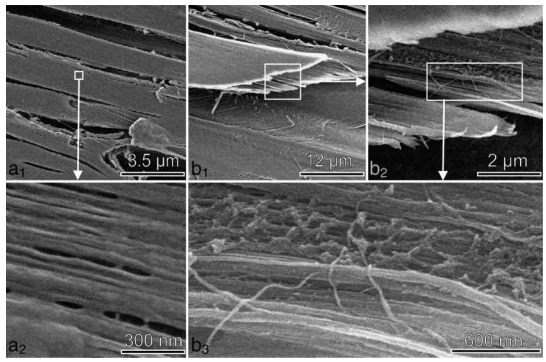

Figure 5. SEM observation of poplar tension wood after critical point drying. (a_2) is a detail of (a_1) showing cellulose aggregates separated by empty spaces. ($b_{1\rightarrow3}$) In between the cellulose microfibrils well-oriented along the fiber, one can observe a fibril network typical of a polysaccharide aerogel structure.

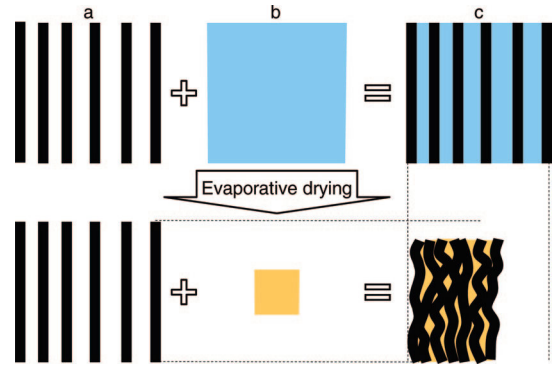

Figure 6. Schematic model of the evaporative drying of G-layer constituents (a, cellulose framework; b, gel phase) and consequences on G-layer shrinkage (c). Constituent proportions and scale are arbitrary.

to present nearly three times the surface area per mass unit of the TW sample, viz., about 48 $m^2\ g^{-1}$. This value corresponds to the surface area of cylindrical fibrils with the density of cellulose (1.5 g cm^{-3}) and an average diameter of 55 nm.

Taking into account the size of cellulose crystallites as measured by Washusen et al.[40] (3.6 nm in TW and 3.2 nm in NW) or Ruelle et al.[41] (3.31 nm in TW and 2.65 in NW) in several species, the fibrils have to be considered as aggregates of cellulose microfibrils. Cellulose aggregate have already been observed and measured: Fahlén and Salmén[42] reported on *Picea abies*, aggregate diameters from 18 to 23 nm depending on processing, and Ruelle et al.[43] reported on *Laetia procera* aggregates smaller in opposite wood than in TW, 18.4 and 21.9 nm, respectively. Recently, Donaldson[44] measured aggregates in poplar and obtained 14 nm in TW G-layer compared to 16 nm in S_2 layer of NW. Thus, compared to the literature, the diameter we calculated (55 nm) appears especially high. As a possible explanation, the dehydration by ethanol could have caused the aggregates to merge into larger aggregates; this would also account for the small but significant macroscopic shrinkage observed at this stage.

If the aerogel obtained by supercritical drying provides a correct image of the texture of the system, the large accessible surface area of the G-layer designates it as a bicontinuous system, formed by a dispersed solid phase and a void volume, which is occupied by water in the wet system. This corresponds to the definition of gel, viz., a system formed by interpenetrating solid and fluid phases. Such an open system is liable to collapse when water is evaporated, as the capillary tension of the water−vapor interface draws the fibrils together. The loss of porosity after evaporative drying confirms this collapse phenomenon.

Observation of longitudinal sections by SEM (Figure 5), indeed shows that cellulose fibrils are organized in primary aggregates parallel to the fiber axis. The size of these aggregates has been measured between 35 and 40 nm, and the space between primary aggregates varies from full contact to more than 55 nm. The observations would be compatible with a layered organization of secondary aggregates and a nonaxisymmetric distribution of the distances between secondary aggregates. In some places, thin filaments nearly 15 nm thick can be observed between parallel aggregates. These filaments present a similar morphology as that commonly observed in aerogel of amorphous polysaccharides.[45,46]

Conclusion

The gel structure identified in the G-layer allows comparison of its behavior to the known structure of other gels. Collapse of the gels during drying, resulting in very high shrinkage, is commonplace[29] and has been observed in other polysaccharidic systems (for example a volume shrinkage exceeding 70% has been measured in alginate[46]). The organization of the cellulose network parallel to the fiber in the G-layer, together with the absence of a reinforcing S_3 layer on its inner boundary (see Figure 1), explains its observed transverse shrinkage of 20% in the cellular context.[39] In the longitudinal direction, the contribution of the cellulose network to prevent gel shrinkage is more difficult to evaluate. However, as shown recently,[28] cellulose microfibrils are not able to restrain the shrinkage induced by drying. Thus, the gel collapse is strong enough to be the driving force of cellulose microfibril buckling (Figure 6). Then the high longitudinal shrinkage of the G-layer is transmitted to the whole fiber thanks to its adhesion to the other layers of the secondary wall[27] to produce a macroscopic longitudinal shrinkage sometimes exceeding 1% in TW.

This discovery is interesting from a materials science standpoint for its relevance to the drying process of wood products. It also opens a new path for biomechanics research to understand how the production of such a gel structure allows very high growth stresses in trees. A better understanding of structural feature and behavior of different types of wood tissues will be helpful to control their consequences and could moreover inspire biomimetical applications in the field of material design. An equally challenging prospect would be to find some added value to wood containing a large proportion of these gelatinous fibers, considering how efficient they are for the tree.

Acknowledgment. Wood samples and the drawing were provided by Pierre Cabrolier, and anatomical sectioning and staining were performed by Francis Mathew (LMGC). The authors thank Jeannine Blanc (LMGC) for her help with the bibliographic research. This research has been performed in the framework of the Woodiversity project supported by the French National Research Agency (ANR). Seminal contacts for this work have been established inside the CNRS-INRA Research Association on Assembly of Plant Molecules (GDR AMV).

References and Notes

(1) Alméras, T.; Thibaut, A.; Gril, J. *Trees* **2005**, *19* (4), 457–467.
(2) Archer, R. R. *Growth stresses and strains in trees*; Springer Verlag: Berlin/Heidelberg/New York, 1986.

(3) Timell, T. E. *Compression wood in gymnosperms*; Springer Verlag: Berlin/Heidelberg/New York, 1986; Vol. 1.
(4) Onaka, F. *Wood Res. (Kyoto, Jpn.)* **1949**, *24* (3), 1–88.
(5) Norberg, P. H.; Meier, H. *Holzforschung* **1966**, *20*, 174–178.
(6) Chaffey, N. *Trends Plant Sci.* **2000**, *5* (9), 360–362.
(7) Ruelle, J.; Clair, B.; Beauchêne, J.; Prevost, M. F.; Fournier, M. *IAWA J* **2006**, *27* (4), 341–376.
(8) Clair, B.; Ruelle, J.; Beauchêne, J.; Prevost, M. F.; Fournier, M., *IAWA J.* **2006**, *27*, (3), 329–338.
(9) Potter, M. C. *Ann. Bot.* **1924**, *18*, 121–140.
(10) Metzger, K. *Naturwiss. Z. Forst- Landwirtsch.* **1908**, *6* (5), 249–273.
(11) Sanio, C. *Bot. Zeitung* **1863**, *21* (13), 101–111.
(12) Sanio, C. *Bot. Zeitung* **1860**, *18* (22), 193–200.
(13) Sanio, C. *Bot. Zeitung* **1860**, *18* (23), 201–204.
(14) Skaar, C. Springer-Verlag: Berlin Heidelberg, 1988; p 283.
(15) Barrett, J. D.; Schniewind, A. P.; Taylor, R. L. *Wood Sci.* **1972**, *4*, 178–192.
(16) Cave, I. D. *Wood Sci. Technol.* **1972**, *6*, 284–292.
(17) Yamamoto, H. *Wood Sci. Technol.* **1999**, *33*, 311–325.
(18) Yamamoto, H.; Sassus, F.; Ninomiya, M.; Gril, J. *Wood Sci. Technol.* **2001**, *35* (1–2), 167–181.
(19) Chow, K. Y. *Forestry* **1946**, *20*, 62–77.
(20) Clair, B.; Ruelle, J.; Thibaut, B. *Holzforschung* **2003**, *57* (2), 189–195.
(21) Clarke, S. H. *J. For.* **1937**, *11* (2), 85–91.
(22) Yamamoto, H.; Abe, K.; Arakawa, Y.; Okuyama, T.; Gril, J. *J. Wood Sci.* **2005**, *51* (3), 222–233.
(23) Boyd, J. D. *Wood Sci. Technol.* **1977**, *11*, 3–22.
(24) Clair, B.; Thibaut, B. *IAWA J.* **2001**, *22* (2), 121–131.
(25) Yamamoto, H. *J. Wood Sci.* **2004**, *50* (3), 197–208.
(26) Clair, B.; Gril, J.; Baba, K.; Thibaut, B.; Sugiyama, J. *IAWA J.* **2005**, *26* (2), 189–195.
(27) Clair, B.; Thibaut, B.; Sugiyama, J. *J. Wood Sci.* **2005**, *51* (3), 218–221.
(28) Clair, B.; Alméras, T.; Yamamoto, H.; Okuyama, T.; Sugiyama, J. *Biophys. J.* **2006**, *91* (3), 1128–1135.
(29) Brinker, C. J.; Scherer, G. *Sol−gel science*; Academic Press: Boston, MA, 1990.
(30) Cansell, F.; Aymonier, C. A.; Loppinet-Serani, *Curr. Opin. Solid State Mater. Sci.* **2003**, *7*, 331–340.
(31) Pierre, A. C.; Pajonk, G. M. *Chem. Rev.* **2002**, *102*, 4243–4265.
(32) Valentin, R.; Molvinger, K.; Brunel, D.; Quignard, F. *New J. Chem.* **2003**, *27*, 1690–1692.
(33) Valentin, R.; Molvinger, K.; Viton, C.; Domard, A.; Quignard, F. *Biomacromolecules* **2005**, *6*, 2785–2792.
(34) Rasband, W. S. *ImageJ*; National Institutes of Health: Bethesda, MD, 1997–2006.
(35) Brunauer, S.; Emmett, P. H.; Teller, E. *J. Am. Chem. Soc.* **1938**, 309.
(36) Rouquerol, F.; Rouquerol, J.; Sing, K. *Adsorption by powders and porous solids: Principles, methodology and applications*; Academic Press: San Diego, CA, 1999.
(37) Broekhoff, J. C. P.; de Boer, J. H. *J. Catal.* **1967**, *9*, 8–14.
(38) Ravikovitch, P. I.; Neimark, A. V. *Langmuir* **2002**, *18*, 9830–9837.
(39) Fang, C.; Clair, B.; Alméras, T.; Gril, J., *Wood Sci. Technol.* **2007**, *41* (8), 659–671.
(40) Washusen, R.; Evans, R. *IAWA J.* **2001**, *22* (3), 235–243.
(41) Ruelle, J.; Yamamoto, H.; Thibaut, B. *BioResources* **2007**, *2* (2), 235–251.
(42) Fahlén, J.; Salmén, L. *J. Mater. Sci.* **2003**, *38* (1), 119–126.
(43) Ruelle, J.; Yoshida, M.; Clair, B.; Thibaut, B. *Trees* **2007**, *21* (3), 45–355.
(44) Donaldson, L. *Wood Sci. Technol.* **2007**, *41*, 443–460.
(45) Serp, D.; Mueller, M.; von Stockar, U.; Marison, I. W. *Biotechnol. Bioeng.* **2002**, *79*, 253.
(46) Valentin, R.; Molvinger, K.; Quignard, F.; Di Renzo, F. *Macromol. Symp.* **2005**, *222*, 93–101.